

## A Sea State Parameterization with Nonarbitrary Wave Age Applicable to Low and Moderate Wind Speeds

MARK A. BOURASSA

*Center for Ocean–Atmospheric Prediction Studies, The Florida State University, Tallahassee, Florida*

DAYTON G. VINCENT

*Department of Earth and Atmospheric Sciences, Purdue University, West Lafayette, Indiana*

W. L. WOOD\*

*School of Civil Engineering, Purdue University, West Lafayette, Indiana*

(Manuscript received 8 March 1999, in final form 23 January 2001)

### ABSTRACT

A simple coupled flux and sea state model is developed. It is applicable to low, moderate, and high wind speeds, with a nonarbitrary wave age. It is fully consistent with an atmospheric flux parameterization. The flux model includes the influence of capillary waves on surface stress, which dominate surface stress on a wave-perturbed surface for  $U_{10} < 7 \text{ m s}^{-1}$ . The coupled model is verified for conditions of local equilibrium and it is used to examine the influences of surface tension and capillary waves on the equilibrium sea state at low and moderate wind speeds ( $U_{10} < 7 \text{ m s}^{-1}$ ). Capillary waves can directly influence characteristics of the airflow (roughness length and friction velocity), and surface tension can directly influence wave characteristics (period, phase speed, and wave age). The influences of capillary waves and surface tension on wave characteristics are found to be noticeable for  $U_{10} < 6 \text{ m s}^{-1}$ , and are likely to be significant in most applications when  $U_{10} < 5 \text{ m s}^{-1}$ . The conditions under which relations valid for higher wind speeds break down are discussed. The new sea state parameterization is an improvement over previous relations (which apply well for  $U_{10} > 7 \text{ m s}^{-1}$ ) because it is also applicable for low and moderate winds. The mean wind speed over most of the world's oceans is less than  $7 \text{ m s}^{-1}$ , so there is considerable need for such a parameterization. The nonarbitrary wave age is particularly important because of the influence of wave age on the shape and size of waves, as well as fluxes of momentum, heat, and moisture.

Additional results include a criterion for the capillary cutoff, significant wave height, and dominant wave period (as functions of wind speed and wave age). Consistency with a flux parameterization is crucial because of the influence of atmospheric stability on surface stress, which influences wave characteristics. The modeled significant wave height for local equilibrium is shown to be consistent with several parameterizations. The modeled dominant period is a good match to that of the Pierson–Moskowitz spectrum when  $U_{10} > 13 \text{ m s}^{-1}$ ; however, for lower wind speeds, the modeled period differs significantly from that of the Pierson–Moskowitz spectrum. The new model is validated with field observations. The differences are largely due to the capillary cutoff, which was not considered by Pierson and Moskowitz.

### 1. Introduction

Recent efforts in wave modeling (Janssen 1989; Günther et al. 1992; Komen et al. 1994) and air–sea flux observations and modeling (Maat et al. 1991; Smith et al. 1992; Perrie and Toulany 1990; Donelan et al. 1997; Bourassa et al. 1999) have shown the need for a non-

arbitrary sea state parameterization as a function of wind speed. Contrary findings have been expressed by Yelland et al. (1998); however, the observations used in that study were not sorted to remove the influences of swell (Bourassa et al. 1999). In practice, the sea state parameters required for flux models are rarely known, and arbitrary assumptions must be made regarding the sea state. For example, one of the most detailed wave models currently in use, WAMS (Wave Model: Günther et al. 1992), requires an arbitrarily assigned wave age. This problem is significant because of the influence of wave age on the shape and size of waves, as well as fluxes of momentum, heat, and moisture. The parameterization of wave age is further complicated by a wide

---

\* Deceased.

---

*Corresponding author address:* Dr. Mark A. Bourassa, Center for Ocean–Atmospheric Prediction Studies, The Florida State University, Tallahassee, FL 32306-2840.  
E-mail: bourassa@coaps.fsu.edu

variety of definitions for wave age [reviews include Donelan (1990)]:  $c_p/u_*$  (Maat et al. 1991; Smith et al. 1992),  $c_p/U_\lambda$  (Stewart 1974),  $c_p/U_{10}$  (Perrie and Toulany 1990),  $c_p/U_{\lambda/2}$  (Donelan 1990), and  $\mathbf{u}_* \cdot \hat{\mathbf{e}}_i/c_{p_i}$  (Bourassa et al. 1999). In these definitions  $c_p$  is the phase speed of the dominant waves,  $u_*$  is the friction velocity,  $U$  is the wind speed at a height equal to the subscript (wavelength of the dominant waves, half that wavelength, or 10 m), and  $\hat{\mathbf{e}}_i$  are basis vectors with components parallel ( $i = 1$ ) and perpendicular ( $i = 2$ ) to the dominant wave's mean direction of propagation. The forms with a wind speed are often applied when an accurate measure of friction velocity is not available. A sea state parameterization (modeling wave age, significant wave height, phase speed of the dominant waves, etc.) for conditions of local wind–wave equilibrium is discussed herein. Capillary waves and surface tension, which dominate atmospheric turbulent surface fluxes for low and moderate wind speeds ( $U_{10} < 7 \text{ m s}^{-1}$ ; Bourassa et al. 1999), are examined in the context of their influence on sea state.

Relations that are often used to calculate  $c_p$  (e.g., Pierson and Moskowitz 1964) and  $u_*$  (e.g., Smith 1980) were developed for moderate and high wind speed conditions ( $U_{10} > 8 \text{ m s}^{-1}$ ), for which surface tension and capillary (surface tension) waves have been considered negligible in comparison to gravity waves (Bourassa et al. 1999). The advantages of the model developed herein are most evident at low and moderate wind speeds ( $U_{10} < 7 \text{ m s}^{-1}$ ), where similarity relations that apply well at greater wind speeds break down (Bourassa et al. 1999). Two causes of this breakdown are the influence of capillary waves on the characteristic of the airflow (roughness length and friction velocity) and surface tension on wave characteristics (period, phase speed, and wave age). Our new sea state model is fully coupled with a surface flux model (Bourassa et al. 1999) that considers atmospheric turbulent mixing due to capillary waves. This flux model is briefly reviewed in section 2b(1). The coupling of the sea state and flux model is self-consistent in a manner that accounts for the three strongest influences on fluxes: wind speed, atmospheric stability, and sea state (i.e., wave age and swell direction). The model will be used to examine the wave age corresponding to local wind–wave equilibrium, and to examine the influence of capillary waves on this wave age.

The theoretical development of the sea state parameterization (section 3), for the couple flux and sea state model, avoids relations that apply only to high wind speeds or gravity waves. The influence of surface tension on significant wave heights is not well known, and the influence of wave age on the capillary cutoff has not previously been examined. For conditions of local equilibrium between the wind and the waves, this cutoff is often described as the wind speed below which waves will not be generated. In section 3c, it will be shown how the phase speed can be used to specify a capillary

cutoff. The model verification includes a check that the model results for high wind speeds are consistent with the accepted relations. The widely accepted observation, that the direct influence of surface tension on wave characteristics is negligible for at least  $U_{10} > 7 \text{ m s}^{-1}$ , is consistent with the coupled model. Modeled wave characteristics are examined for low and moderate wind speeds, to determine for which conditions the similarity relations that apply for  $U_{10} > 7 \text{ m s}^{-1}$  break down. It will be shown that surface tension and capillary waves are important to most applications for  $U_{10} < 5 \text{ m s}^{-1}$ . For  $U_{10} < 13 \text{ m s}^{-1}$  the modeled period differs significantly from that of the Pierson–Moskowitz (P–M) spectrum. The model results are shown to be a close match to observations (section 4b). The differences are largely due to the capillary cutoff, which was not considered by Pierson and Moskowitz. Applications that require wave characteristics for low and moderate wind speed conditions are expected to greatly benefit from this result.

## 2. Background

There has been a tendency to dismiss capillary waves as too small (compared to gravity waves) to contribute to the surface roughness (Hay 1955; Miles 1957). For high wind speeds, this argument is probably valid; there is no evidence that capillary waves need be directly considered in parameterizations of roughness length ( $z_o$ ) for  $U_{10} > 7 \text{ m s}^{-1}$ . The contribution to roughness length from one capillary wave is certainly negligible compared to an individual gravity wave; however, the roughness length of a surface is related to the sum of contributing roughness elements (i.e., waves). There are many capillary waves for each gravity wave; the ratio of wavelengths (and hence density) is typically greater than  $10^4:1$ . When superposition and the crossflow direction are considered the ratio can be  $10^7:1$ . Individual capillary waves do not have to make much of a contribution to roughness length for capillary waves to contribute to a large fraction of the roughness length (Bourassa et al. 1999).

The background begins with a short review of how waves are influenced by the vertical wind profile. The rest of the background is divided into two sections: the influence of capillary waves on the shape of the wind profile, and the influence of surface tension on wave characteristics. These considerations are linked through the wave age parameterization, which is developed in section 3, for use in the coupled flux and sea state model. A key to correctly coupling the flux and sea state models is an accurate determination of the friction velocity, which appears in parameterizations for the vertical profile of wind speed, wave age, surface stress, atmospheric stability, and significant wave height.

### a. Link between the wind profile and waves

There have been many studies linking wave characteristics such as amplitude and phase speed to the wind

TABLE 1. The physical considerations in the roughness length parameterizations of Charnock (1955), Smith et al. (1992), a variation of Smith (1988), and Bourassa et al. (1999).

	Charnock	S92	S88	BVW
Gravity waves	yes	yes	yes	yes
Capillary waves	no	no	no	yes
Aerodynamically smooth	no	no	yes	yes
Surface wave age	no	yes	yes	yes
Two horizontal dimensions	no	no	no	yes

profile. The Miles (1957) theory is one such commonly accepted wave generation model based on form drag. Such models consider the wind speed passing immediately over the wave as equal to the wave's phase speed. If this condition is met, air pressure fluctuations are in phase (resonance) with the water surface, and the growth mechanism is as described by Jeffereys (1925). Typically this theory is applied to each frequency component of the wave field. This approach allows a complicated wave field to be considered; however, it is computationally expensive (Janssen 1991). There have been numerous attempts to apply variations of the Miles theory to modeling wave fields (Phillips 1977; Janssen 1982, 1989, 1991; Jenkins 1992) and surface stresses (Miles 1957; Janssen 1991; Jenkins 1992, 1993).

An alternative approach to linking waves and a wind profile is to solve the nonlinear hydrodynamic equations with the application of turbulence closure schemes (Chalikov 1978, 1986; Makin 1980, 1982, 1987; Makin and Panchenko 1986; Chalikov and Makin 1991). This approach and the Miles theory require a model for the wind profile. The physics describing the shape of the wind profile over water waves is a matter of ongoing research. However, there have been recent improvements in modeling stresses for low and moderate wind speeds, which bring together in situ and wave-tank observations in a consistent manner and apply to two (horizontal) dimensions (Bourassa et al. 1999). We build upon these results (summarized below) in the development of our model.

#### b. The influence of capillary waves on characteristics of the airflow

Our original interest in the sea state problem arose from attempts to develop accurate flux parameterizations for a wide variety of wind and sea conditions. Consequently, one requirement was that the sea state parameterization be fully compatible with the parameterization of the momentum flux. The downward momentum flux ( $\tau$ ) can be modeled in terms of the friction velocity ( $\mathbf{u}_*$ ):

$$\tau = \rho \mathbf{u}_* |\mathbf{u}_*|, \quad (1)$$

where  $\rho$  is the density of the air. The friction velocity is also a key parameter in determining the wind profile. The magnitude of the friction velocity depends on the

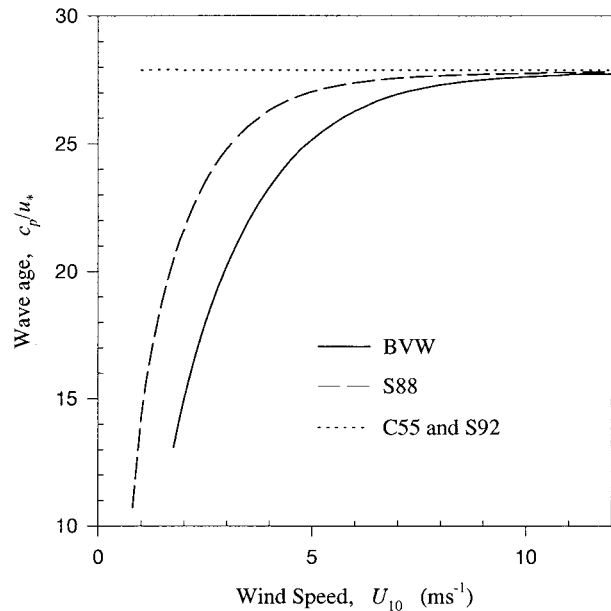


FIG. 1. Wave age as a function of  $U_{10}$  determined by Eq. (14) with four roughness length parameterizations.

wind speed and the roughness length ( $z_o$ ) of the surface. For low and moderate wind speeds ( $U_{10} < 7 \text{ m s}^{-1}$ ), capillary waves can make a large contribution to this roughness length (Wu 1968; Bourassa et al. 1999), and largely determine the value of the friction velocity.

The direct influence of capillary waves on flux and airflow characteristics ( $\mathbf{u}_*$  and  $z_o$ ) is determined by the relation between  $\mathbf{u}_*$  and  $z_o$ . Given  $z_o(\mathbf{u}_*)$  and the modified log-wind relation  $\mathbf{U}(z)$ , it is possible to iteratively solve for  $\mathbf{u}_*(\mathbf{U})$  and  $\tau(\mathbf{U})$ . The modified log-wind relation is

$$\mathbf{U}(z) - \mathbf{U}_s = \frac{\mathbf{u}_*}{\kappa} \left[ \ln \left( \frac{z}{z_o} + 1 \right) + \varphi(z, z_o, L) \right], \quad (2)$$

where  $\mathbf{U}_s$  is the mean surface current,  $z$  is the mean height above the surface,  $\kappa$  is von Kármán's constant,  $\varphi$  is the atmospheric stability term, and  $L$  is the Monin–Obukhov scale length (a measure of atmospheric stability in the boundary layer). The Bourassa–Vincent–Wood flux model (BVW: Bourassa et al. 1999) uses the stability parameterizations of Beljaars and Holtslag (1991) for stable air, and Benoit (1977) for unstable air. The value of  $z_o$  is dependent on the choice of frame reference ( $\mathbf{U}_s$ ; Bourassa et al. 1999), which (in the BVW model) is the local mean surface current.

#### 1) ROUGHNESS LENGTH PARAMETERIZATIONS

Four dimensionally sound roughness length parameterizations will be contrasted to illustrate key physical concepts: Charnock (1955), Smith (1988), Smith et al. (1992), Bourassa et al. (1999). These parameterizations

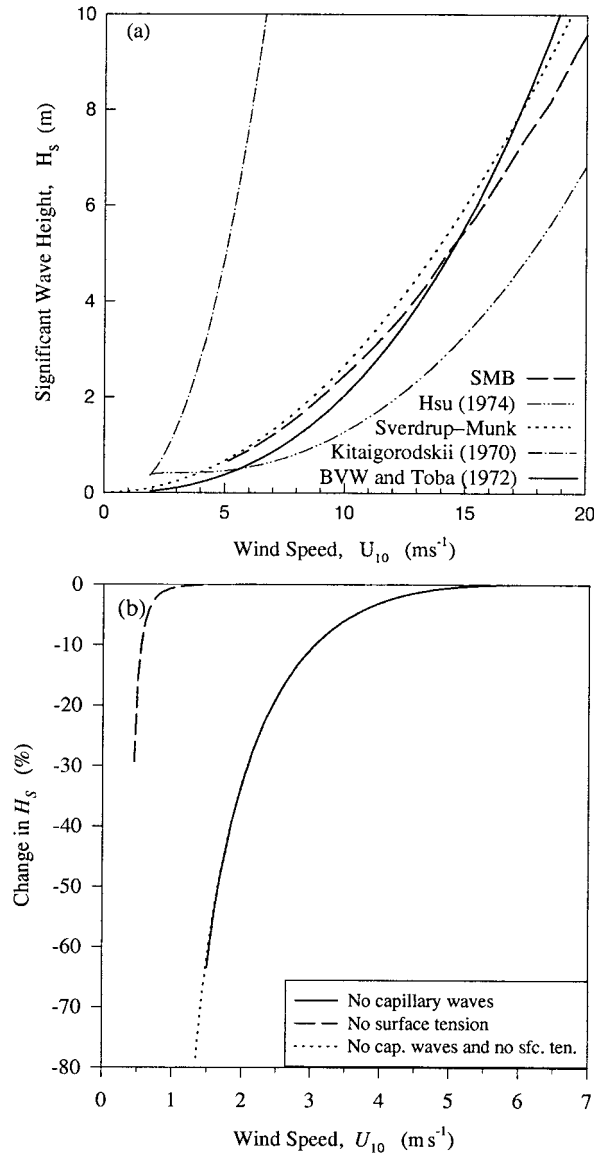


FIG. 2. Significant wave height modeled with our sea state parameterization (a) compared to estimates from other observationally based parameterizations, and (b) demonstrating the importance of capillary waves in the roughness length (dashed and solid lines) and surface tension in the phase relation (dotted and solid lines).

consider different sets of influences (Table 1) in the relation between  $u_*$  and  $z_o$ . Charnock's (1955), is the simplest of these roughness length parameterizations:

$$z_o = au_*^2/g, \tag{3}$$

where  $a = 0.185$  (Wu 1980) is an empirically derived constant. Only gravity waves are considered to contribute to the roughness length, and  $z_o$  is independent of sea state. Charnock considered that  $z_o$  could be dependent on sea state; however, he lacked the appropriate data to test such a hypothesis. Recently, there have been

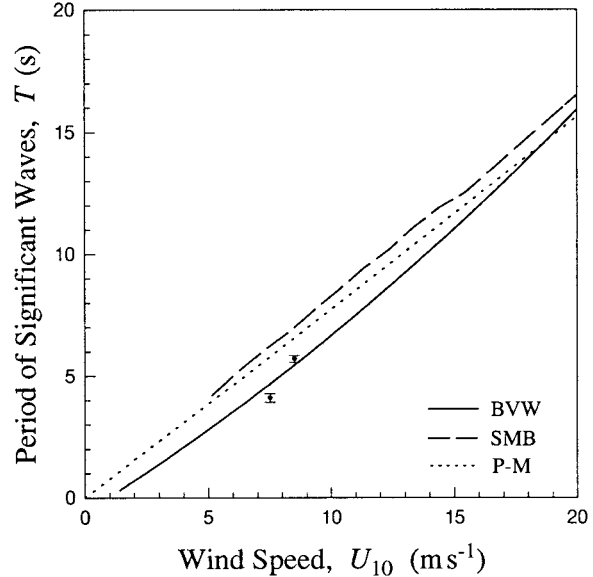


FIG. 3. Period of the dominant waves modeled with our sea state parameterization compared to estimates from other observationally based parameterizations. The dots are binned open ocean observations from SCOPE and SWADE, in  $\sim 2 \text{ m s}^{-1}$  bins (seven and eight observations per bin), for wave ages between 22 and 35. The error bars indicate one standard deviation from the mean within the bin. The mean wave age in the higher wind speed bin is  $>28$  (the equilibrium value), consistent with an overestimation of  $T_p$ . The mean wave age in the lower wind speed bin is  $<28$ , consistent with an underestimation of  $T_p$ .

several examinations of the dependence of Charnock's constant ( $a$ ) on the sea state (Kusaba and Masuda 1988; Geernaert et al. (1986); Toba et al. 1990; Perrie and Toulany 1990; Maat et al. 1991; Smith et al. 1992; Yelland et al. 1998), for which Smith et al. (1992, thereafter S92) found

$$z_o = \frac{0.48 u_*^2}{w_a g}, \tag{4}$$

where  $w_a = c_p/u_*$  is wave age. This finding applied only in the absence of swell, when the mean wind and waves were moving in parallel directions. There are several controversies regarding this finding for these highly restrictive conditions (Yelland et al. 1998; Bourassa et al. 1999). Toba et al. (1990) combined field and wave tank data to develop an alternative relation where  $z_o \propto w_a$ . Further discussion of this result can be found in Donelan et al. (1993). In S92 gravity waves are the only roughness elements; the improvement over Charnock's relation is the consideration of nondirectional sea state (i.e., wave age).

Both of the above roughness length parameterizations are based upon observations with  $U_{10} > 6 \text{ m s}^{-1}$ , and are not adequate at low and moderate wind speeds. Smith (1988, hereafter S88) attempted to rectify this shortcoming though consideration of the mixing induced by an aerodynamically smooth surface in addition to that induced by gravity waves (in this case there were

only three observations with  $U_{10} < 8 \text{ m s}^{-1}$ ). He assumed that the roughness length for an aerodynamically smooth surface (Nikuradse 1933; Kondo 1975; Brutsaert 1982) could be added linearly to the gravity wave roughness length:

$$z_o = \frac{0.11\nu}{u_*} + \frac{0.48}{w_a} \frac{u_*^2}{g}, \quad (5)$$

where  $\nu$  is the molecular viscosity. Smith (1988) used a constant value of Charnock's "constant," rather than the wave-age-dependent form in S92 and Eq. (5) herein; S88 refers to hybrid parameterization (5) considering both light winds and sea state. This parameterization is valid when gravity waves dominate the flow ( $U_{10} > \sim 7 \text{ m s}^{-1}$ ) and when the surface is aerodynamically smooth ( $U_{10} < \sim 2 \text{ m s}^{-1}$ ). It would also be valid for the intermediate wind speeds if capillary waves made a negligible total contribution to the roughness length. Bourassa et al. (1999) showed that the S88 roughness length was too small (for aerodynamically rough surfaces) at moderate wind speeds ( $\sim 2 < U_{10} < 7 \text{ m s}^{-1}$ ) and applied wave tank observations to develop a capillary wave roughness length, which lead to improved matches to observed fluxes. The key aspects of the BVW model are summarized as follows. The roughness length is modeled as the weighted root-mean-square sum of roughness lengths for gravity waves, capillary waves, and an aerodynamically smooth surface (respectively indicated by subscripts of  $g$ ,  $c$ , and  $s$ ). The weighting terms ( $\beta'$  and  $\beta$ ) consider whether or not the type of wave is present ( $\beta'$ ), as well as shifts in the velocity frame of reference due to the orbital motion of gravity waves ( $\beta_c$ ):

$$z_{oi} = \left[ \left( \beta_s \frac{0.11\nu}{|\mathbf{u}_{*i}|} \right)^2 + \left( \beta'_c \beta_c \frac{b\sigma}{\rho |\mathbf{u}_{*i}| |\mathbf{u}_{*i} \cdot \hat{\mathbf{e}}_i|} \right)^2 + \left( \beta'_g \frac{0.48}{w_{ai}} \frac{|\mathbf{u}_{*i}| |\mathbf{u}_{*i} \cdot \hat{\mathbf{e}}_i|}{g} \right)^2 \right]^{0.5}. \quad (6)$$

The unit vectors  $\hat{\mathbf{e}}_i$  are two perpendicular basis vectors,  $\sigma$  is surface tension,  $\rho_w$  is the density of water,  $b = 0.06$  is a dimensionless constant, and  $g$  is gravitational acceleration. Sea state enters (6) through the wave age ( $w_a$ ), shifts in the velocity frame of reference ( $\beta_c$ ), and the capillary cutoff (through  $\beta'_c$ ). For point fluxes over an aerodynamically smooth surface  $\beta_g = \beta_c = 0$  and  $\beta_s = 1$ . The main difference between the BVW model and the S88 model applicable herein is the consideration of capillary waves.

The considerations in these four roughness length parameterizations are summarized in Table 1. The range of conditions to which the models are applicable increases from left to right. These are increasingly detailed methods for determining the friction velocity.

## 2) SUMMARY OF THE DEPENDENCE OF FRICTION VELOCITY ON WAVE AGE

Of the four roughness length parameterizations described above (and in Table 1), only Charnock's is independent of wave age; the other three parameterizations require that wave age be known through theory or observation. The friction velocity can be determined given wave age, Eq. (2), and the corresponding equations for air temperature and moisture (which are used to determine the atmospheric stability parameter  $L$ ) (Liu et al. 1979; Bourassa et al. 1999), one of Eqs. (3) to (6), and typical field observations (wind velocity, sea surface temperature, air temperature, and a measure of atmospheric moisture). The BVW calculation for  $\mathbf{u}_*$  is also dependent on the angle between the mean wind direction and the propagation direction of the dominant waves. This angle is equal to zero for conditions of local wind-wave equilibrium. The influence of this angle on fluxes has recently been discussed in terms of observations (Donelan et al. 1997) and modeling (Bourassa et al. 1999). Hereafter, the discussion will be simplified by assuming that the mean wind is parallel to the direction of wave propagation.

### c. Influence of surface tension on wave characteristics

The relation between phase speed ( $c_p$ ) and period ( $T_p$ ) of the significant waves and surface tension ( $\sigma$ ) is given in the phase relation for surface water waves:

$$c_p = \frac{gT_p}{2\pi} + \frac{2\pi\sigma}{T_p\rho_w}, \quad (7)$$

where  $\rho_w$  is the density of water. For applications restricted to long periods (equivalent to long wavelengths), the surface tension term is often dropped; however, the surface tension term will be retained herein. It will be important in determining our capillary cutoff and in examining the influence of surface tension for moderate wind speeds. The phase relation can be written as a second-order polynomial in  $T_p$ . The positive root of this quadratic equation is the period of the significant waves (opposed to the period of capillary waves with the same phase speed):

$$T_p = \frac{\pi}{g} \left( c_p + \sqrt{c_p^2 - c_{p\min}^4/c_p^2} \right), \quad (8)$$

where  $c_{p\min} = (4g\sigma/\rho_w)^{1/4} \approx 23.2 \text{ cm s}^{-1}$  is the minimum phase speed for surface waves.

Most wave applications, such as spectral wave models, determine the dominant wave period from the Pierson-Moskowitz relation:

$$T_p = 7.1U_{19.5}/g. \quad (9)$$

The relationship between wind speed and the  $T_p$  developed by P-M was based on Kitaigorodskii's (1961) relation between frequency ( $T^{-1}$ ) and friction velocity.

Pierson–Moskowitz assumed (seemingly reasonably at the time) that the wind speed at a height of 19.5 m is directly proportional to the friction velocity, and that the proportionality is constant. This assumption implies that the drag coefficient is independent of wind speed, which is no longer considered to be a reasonable approximation (reviews include Donelan 1990).

The P–M relation was developed for waves in approximate equilibrium with winds for the range from  $U_{10} = 10.3$  to  $20.6 \text{ m s}^{-1}$  (20 to 40 kt), rather than waves associated with low and moderate winds ( $U_{10} < 7 \text{ m s}^{-1}$ ). This limitation of (9) is rarely stated in descriptions of wave models that utilize (9). Pierson–Moskowitz chose the best linear fit of the observed  $T_p(U_{19.5})$ , assuming that the line passed through the origin. Consequently, the period in (9) approaches zero as the wind speed approaches zero. This approximation conflicts with observations that the capillary cutoff occurs in the range of  $1 < U_{10} < 4 \text{ m s}^{-1}$  (Ursell 1956).

### 3. Model development

In order to determine the period as a function of wind speed and sea state, the phase speed is described in terms of wave age (hereafter wave age will refer to the  $c_p/u_{*}$  form) and friction velocity:

$$c_p = u_* w_a. \quad (10)$$

This has rarely been done because most applications determine wave age from  $c_p$  and  $u_*$ ; however, it has the advantage of allowing wave and atmospheric flow characteristics to be parameterized in terms of wave age and wind speed.

The sea state is often described in terms of wave age, which is a first-order approximation of the equilibrium sea state (Huang et al. 1990). By convention, a sea with a small wave age is called a young sea. For strong wind conditions, a young sea is usually a growing sea. Conversely, a sea with decaying waves has a large wave age and is called an old sea. Swell from distant storms is an example of an old sea. One purpose of the sea state parameterization presented herein is to determine local-equilibrium values of wave age and other wave characteristics (e.g., significant wave height) as a function of wind speed. For conditions of local equilibrium and 10-m winds in excess of  $10 \text{ m s}^{-1}$ , the wave age determined from observations has been found to be between 26 and 28 (Donelan 1990). Wave age is not a complete description of the wave field, even as a first-order approximation (Huang et al. 1990). Donelan's description of wave age for  $U_{10} > 10 \text{ m s}^{-1}$  required a statement regarding wave field growth and decay. Therefore, wave age will be modeled as a function of wind stress and a growth term. Regrettably, it is beyond the scope of this article to develop a model of wave evolution (i.e., the rate of change of the growth term). However, the effects of wave growth and decay con-

ditions on modifying drag coefficients have been shown in Bourassa et al. (1999).

The new sea state parameterization has several similarities with the Miles (1957) model of wave growth. The BVW sea state parameterization can be used to describe departures from a condition of local wind–wave equilibrium. However, due to a lack of sufficient observations to test the model for nonequilibrium conditions, the focus of this study is the sea state for local wind–wave equilibrium. A wave field is considered to be in local equilibrium with the mean wind when all probability density functions describing the wind and wave characteristics are constant with respect to time (provided a sufficiently long averaging period). Most applications of the Miles theory considered the mean wind speed passing over the top of each Fourier component of the wave field, and related this wind speed to the phase speed of these components. In contrast, our sea state model considers the mean wind speed at the significant wave height, and considers only the frequency corresponding to the dominant waves. This approach is far less computationally demanding than considering a wide range of frequencies, as is done in the WAMS model (Günther et al. 1992; Janssen 1989, 1991). Clearly our model cannot be applied to highly complicated sea states; however, it will be shown to work well for local equilibrium conditions and to qualitatively explain physics for nonequilibrium conditions. The sea states that can be modeled (or well approximated) using this model are much more diverse than can usually be considered with flux models. For example, in the BVW flux model, swell can be specified from one direction while local equilibrium is specified in a perpendicular direction.

The log-wind profile does not apply within several significant wave heights of the surface (Large et al. 1995; Bourassa et al. 1999); however, the log-wind relation (2) can be extrapolated to the significant wave height ( $H_s$ ). This mean wind speed is split into two components: the speed needed for local equilibrium  $U_{\text{eq}}(H_s)$  and a perturbation component  $U_{\text{ne}}(H_s)$ :

$$U(H_s) = U_{\text{eq}}(H_s) + U_{\text{ne}}(H_s). \quad (11)$$

This equation is transformed into a convenient nondimensional form by subtracting the (extrapolated) mean wind speed at the lower boundary (i.e., the mean surface current), and by dividing the difference by the phase speed of the dominant waves:

$$\frac{U(H_s) - U_s}{c_p} = \frac{U_{\text{eq}}(H_s) - U_s}{c_p} \left( 1 + \frac{U_{\text{ne}}(H_s)}{U_{\text{eq}}(H_s) - U_s} \right). \quad (12)$$

To at least a first-order approximation, the term  $[U_{\text{eq}}(H_s) - U_s]/c_p$  is constant (Kitaigorodskii 1970). This term will be referred to as the wind–wave equilibrium term ( $G$ ); the value of  $G$  will be determined in section 3b. The surface speed  $U_s$  is retained in Eq. (12) because it

can be significant in field applications (Chou 1993), and because of the added elegance of making  $G$  and the term in brackets invariant throughout Newtonian frames of reference. The convenience of a constant parameter is a key reason for the choice of  $U(H_s)$ , rather than the mean wind speed at a different height. Another reason for choosing this height is that wave age is a description of the dominant gravity waves and, hence, can be expected to be related to  $H_s$ .

The term in brackets on the right-hand side of (12) is related to local equilibrium, or a lack thereof, and will be referred to as the wind-wave stability term ( $W$ ). A value of  $W > 1$  ( $U_{ne} > 0$ ) indicates a mean wind speed greater than that needed for local wind-wave equilibrium, which is a growth condition. Conversely, a value of  $W < 1$  ( $U_{ne} < 0$ ) indicates insufficient wind to maintain the wave field, which is a decay condition. In summary:

$$W = \begin{cases} >1, & \text{a growing wave field} \\ =1, & \text{local equilibrium} \\ <1, & \text{a decaying wave field.} \end{cases} \quad (13)$$

The wind-wave stability parameter ( $W$ ) can be expressed in terms of wave age by substitution of (12) into (2), and replacement of  $c_p/u_*$  with wave age  $w_a$ :

$$w_a = \frac{1}{\kappa GW} \left[ \ln \left( \frac{H_s}{z_o} + 1 \right) + \varphi(H_s, z_o, L) \right]. \quad (14)$$

In order to use (14) to determine wave age, it is necessary to determine the significant wave height without introducing new unknowns.

#### a. Wave height relations

There are a wide variety of parameterizations for wave height (Kitaigorodskii 1970; Toba 1972; Hsu 1974; Günther et al. 1992; reviews include Haung et al. 1990). The WAMS model (Günther et al. 1992) was not used in the new sea state parameterization because it was too computationally expensive and explicitly did not consider the effects of atmospheric stability on the wind profile. The WAMS model was inconsistent with the goal of a sea state parameterization that is fully compatible with the flux parameterization. Near the surface, the wind velocity modifications due to atmospheric stability are relatively large and should not be ignored (Stull 1988). Toba's parameterization (15) was favored over Kitaigorodskii's (1970) and Hsu's (1974) relations because it is based on parameters that are usually more accurately determined from observations, that is,  $H_s$ ,  $u_*$ , and the period of the dominant waves ( $T_p$ ), rather than  $z_o$ ,  $c_p$ , and the root-mean-square surface displacement:

$$H_s = B(gu_*T_p^3)^{0.5}, \quad (15)$$

where  $B = 0.602$  is an empirically derived constant and

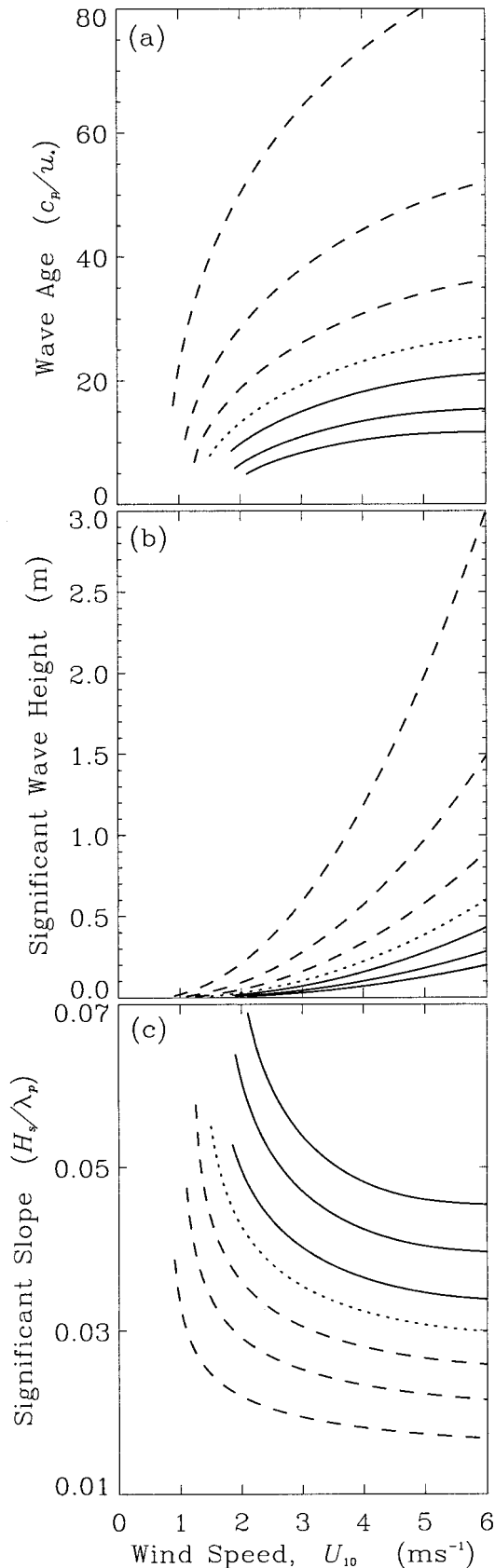
$g$  is gravitational acceleration. The period ( $T_p$ ) can be determined through (8), and friction velocity can be determined from (2) and (6). This significant wave height can then be used to iteratively solve (14).

#### b. The wind-wave equilibrium parameter

There are few studies of wind speed as a function of vertical and horizontal position relative to wave crests (Kawai 1981, 1982; Csanady 1985). Due to difficulties in making these measurements in turbulent flows, there has been little progress in developing theoretically sound models of the mean velocity field. Therefore, the parameter  $G$  is determined indirectly through more easily observed phenomena. For local equilibrium and  $U_{10} - U_s > 10 \text{ m s}^{-1}$ , it is assumed that  $w_a$  is constant. For these conditions, the value of  $G$  is solely dependent on the functionality of the roughness length for gravity waves. For conditions of wind-wave equilibrium, a neutrally stable atmosphere, and  $U_{10} - U_s > 10 \text{ m s}^{-1}$ , wave age has been observed to reach a plateau with a value between 26 and 28 (Donelan 1990). The wave ages derived from Eq. (14) are consistent with this observation when  $\kappa G$  is between 0.32 ( $w_a = 28$ ) and 0.34 ( $w_a = 26$ ). A value of  $G = 0.81$  was chosen to be consistent with  $\kappa = 0.4$  and the popular approximation that the value of the saturation wave age is 28. Some cautions should be expressed regarding this result, as it is dependent on the Humidity Exchange Over the Sea (HEXOS) result (S92), which has been questioned (Yelland et al. 1998; Bourassa et al. 1999). The HEXOS result is used in the absence of a better evaluation of the sea state dependence, and it appears to work well for the restrictive conditions for which it applies, as well as old seas [for which the sea state is dominated by  $\beta'_c$  (Bourassa et al. 1999)]. The above results can be used to determine the local equilibrium values of  $w_a$ , as functions of wind speed, for the S88, S92, and BVW parameterizations (Fig. 1). The consideration of wave age and non-gravity-wave terms (in  $z_o$ ) causes  $w_a$  to increase as  $U$  increases, until  $w_a$  reaches values where it is independent of  $U$ .

#### c. Capillary cutoff

Both field and wind tunnel observations show that, for conditions of local equilibrium, there is a low wind speed cutoff below which neither capillary nor gravity waves exist. This is usually observed in the range of 1–4  $\text{m s}^{-1}$  (Ursell 1956). Observations have shown that ultragravity waves (with both gravity and surface tension contributing to the restoring force) are generated prior to capillary waves. For local equilibrium conditions, we have assumed that neither type of surface wave exists if the modeled phase speed of the dominant waves is less than the minimum phase speed for water waves (i.e., ultragravity waves):



$$u_* W_a \begin{cases} > c_{p\min}, & \text{surface waves exist,} \\ < c_{p\min}, & \text{surface waves do not exist.} \end{cases} \quad (16)$$

The actual minimum phase speed associated with the cutoff is likely to be greater than the minimum phase speed of water waves; consequently this constraint underestimates the phase speed and wind speed associated with the cutoff. However,  $\partial c_p / \partial U_{10} \gg 1$  near the capillary cutoff. Consequently, the error in the wind speed associated with the cutoff is small.

The capillary cutoff is used to distinguish between aerodynamically smooth and rough surfaces. This is an important distinction because the stress over a rough surface is much greater than that over a smooth surface (Byushev and Kuznetsov 1969; Bourassa et al. 1999). The low wind speed cutoff is also useful computationally because it eliminates any chance of Eq. (8) producing a complex number for the period of the dominant waves.

The value of the capillary cutoff is highly dependent on the relation between roughness length and friction velocity. The wave ages determined from the four roughness length parameterizations for conditions of local equilibrium and neutral atmospheric stability are shown in Fig. 1. The greatest differences in modeled wave ages occur at low and moderate wind speeds: the C55 and S92 parameterizations indicate that the equilibrium wave age is approximately constant with wind speed, whereas the other parameterizations are consistent with observations (Donelan 1990) in predicting smaller wave ages for smaller wind speeds. However, the small wave ages modeled with S88 are smaller than observed in field conditions (Ursell 1956; Donelan 1990). The low wave ages predicted with the S88 parameterization are similar to those predicted with the BVW parameterization; the major difference between these two predictions is the range of wind speeds over which the equilibrium value drops. This range is dependent on the magnitude of the roughness length component(s) other than gravity waves. For neutral atmospheric stability and local equilibrium, the capillary cutoff of S88 is  $0.8 \text{ m s}^{-1}$ , which is unrealistically low. The capillary cutoff for BVW is  $U_{10} = 1.8 \pm 0.05 \text{ m s}^{-1}$  (for a water temperature of  $20^\circ\text{C}$ ), which is within the more commonly accepted range (Ursell 1956).

#### 4. Results

Several model results can be verified in comparisons to existing, observation-based, parameterizations. The modeled significant wave height and period of the dom-

←

FIG. 4. Modeled wave field characteristics for various values of  $W$ : (a) wave age, (b) significant height, and (c) significant slope. Dotted line shows local equilibrium, solid lines indicate rising seas, and dashed lines show falling seas.

inant waves are examined (as functions of  $U_{10}$ ) for conditions of local equilibrium ( $W = 1$ ) and neutral atmospheric stability ( $L^{-1} = 0$ ). The impact (on  $H_s$ ) of capillary waves in the roughness length (6) and surface tension in the phase relation (7) are also examined to demonstrate the relative importance of these considerations. These considerations are examined by comparing the output of the unmodified model to cases where  $\beta'_c = 0$  and/or  $c_{p\min} = 0$ .

#### a. $H_s(U_{10})$ for local equilibrium

Observations of  $H_s$  and  $U_{10}$  are the basis of the Sverdrup–Munk, theory and the Sverdrup–Munk–Bretshneider (SMB) nomogram. Sverdrup–Munk theory (S–M) is a best fit between observations of  $H_s$  and  $U_{10}$ :

$$H_s = 2.667 \times 10^{-4} U_{10}^2. \quad (17)$$

The modeled  $H_s(U_{10})$  is similar to the S–M curve and the SMB nomogram (Fig. 2a). The model predicts slightly smaller amplitude waves than the SMB nomogram for  $U_{10} < 15 \text{ m s}^{-1}$  and slightly greater amplitude waves for greater winds. The differences with S–M theory could simply be due to forcing the S–M  $H_s(U_{10})$  to a dimensionally sound polynomial relation (i.e.,  $H_s \propto U_{10}^2/g$ ).

By definition, the model results also match Toba's (1972) parameterization. The wave height parameterizations of Kitaigorodskii (1970) and Hsu (1974) are also shown (Fig. 2a). Kitaigorodskii's relation

$$\sigma = 13.3z_o \exp(\kappa c_p/u_*') \quad (18)$$

(where  $H_s = 4\sigma$  and  $\sigma$  is the rms wave height) models wave heights that are much greater than the other parameterizations. This problem with Kitaigorodskii's relation has been previously observed. In contrast, Hsu's relation

$$\sigma = 1.57z_o(c_p/u_*')^2 \quad (19)$$

has lower significant wave heights than the other parameterizations. The differences in modeled  $H_s$  among Kitaigorodskii's, Toba's, and Hsu's parameterizations are large, but they could be accounted for as systematic errors in the calculation of  $z_o$  (Bourassa et al. 1999; Bourassa 2000), as well as other systematic errors reviewed by Donelan (1990). Toba's choice of parameters greatly reduced the magnitude of systematic errors, as indicated by the similarity between the wave heights modeled by his parameterization (in the BVW sea state parameterization), and those in the observation-based Sverdrup–Munk theory.

The significance of capillary waves and surface tension (in the phase relation) on significant wave height is shown in Fig. 2b. Clearly, they are only significant for low and moderate wind speeds ( $U_{10} < 4 \text{ m s}^{-1}$ ). Surface tension in the phase relation causes the nonzero minimum in phase speed, which is a key component in the capillary cutoff. Surface tension (considered in the

solid and dashed lines) results in a large percentage drop in  $H_s$  as  $U_{10}$  approaches the capillary cutoff. When stress due to capillary waves is not considered (dashed line) this reduction can exceed 70% of  $H_s$  based solely on gravity waves, and it can exceed 60% when capillary waves are also considered (solid line). This problem is further complicated by the dependence of the capillary cutoff on the sea surface temperature, which is considered in the model but will not be discussed further herein. Stress related to capillary waves, without considering the surface tension in the phase speed (dotted line), is only significant for  $U_{10} < 0.5 \text{ m s}^{-1}$ . The resulting  $H_s(U_{10})$  is incompatible with the many observations that the capillary cutoff occurs near the 2–4  $\text{m s}^{-1}$  range. The consideration of surface tension in the phase relation is largely responsible for the differences from models based solely on gravity waves and for this model's reasonable capillary cutoff.

#### b. $T_p(U_{10})$ for local equilibrium

The period of the modeled waves (Fig. 3) differs significantly from those given by the Sverdrup–Munk–Bretshneider nomogram and the Pierson–Moskowitz (1964) spectrum. For  $U_{10} < 13 \text{ m s}^{-1}$  the BVW period is approximately one second less than that predicted by the SMB nomogram. For  $U_{10} < 7 \text{ m s}^{-1}$ , the P–M period is similar to that of the nomogram. The differences are physically significant, and of great interest because the P–M spectrum is the basis of many spectral models of waves (Kitaigorodskii 1970; Hasselman et al. 1976) for conditions near local equilibrium. The P–M assumptions that  $U_{19.5}$  was in constant proportion to the friction velocity, and that the period approaches zero as the wind speed approaches zero, lead to errors for low and moderate wind speeds where the validity of these assumptions breaks down. If the P–M relation was adjusted to pass through  $(T_{\text{cutoff}}, U_{\text{cutoff}})$ , rather than through the  $(T, U)$  origin, the P–M periods would be reduced and be much more similar to the model developed herein.

The assertion that the errors are in P–M rather than BVW is supported by a comparison (Fig. 3a) to field observations (Fairall et al. 1996; Donelan et al. 1997). The San Clemente Ocean Probing Experiment (SCOPE: Fairall et al. 1996) observations were taken from the Scripps Institute Floating Instrument Platform, R/P *FLIP*, in deep water off the California coast. Phase speeds were determined through pressure sensors, and friction velocity was calculated through the inertial dissipation method (as well as other techniques). These observations are used to calculate wave age and select near-equilibrium conditions ( $22 < c_p/u_*' < 35$ ). The period of the dominant waves was calculated through (8) and averaged within the 2  $\text{m s}^{-1}$  wind speed bin within which most of the observations fell. Observations from the Surface Wave Dynamics Experiment (SWADE: Donelan et al. 1997) in deep water off eastern Cape Henlopen and Cape Hatteras included directional wave

spectra that were used to isolate wind-driven seas. Phase speeds of the dominant waves were provided by W. Drennan (2000, personal communication). Friction velocities were determined through eddy correlation and inertial dissipation methods, and the phase speeds were determined from a wave staff array. The periods (averaged over the range of wave ages;  $22 < c_p/u_* < 35$ ) from these field experiments show that P–M overestimates the period for wind speeds near 7 and 9 m s<sup>-1</sup>, and the sea state model developed herein is a much better match to the observations.

## 5. Discussion

The dependency of several wave characteristics on conditions of wave growth and decay will be discussed in this section. The model results are qualitatively consistent with observations. Variations in the capillary cutoff are also examined in section 5a, and variations in wave shape and drag coefficient are examined in section 5b.

### a. Dependence of capillary cutoff on $W$

The wave age (Fig. 4a) shows a change in the capillary cutoff as a function of  $W$ . The values of  $W$  shown are 0.4, 0.6, 0.8, 1.0 (dotted line), 1.2, 1.5, 1.8, with rising sea indicated by solid lines, and falling seas indicated by dashed lines. This finding is consistent with observations that the capillary cutoff for rising seas is greater than that for decaying waves (M. A. Donelan and W. J. Plant 1997, personal communication). The BVW flux model, which considers stress related to capillary waves, has large differences in roughness length associated with the transition between aerodynamically smooth and rough surface. The modeled changes are related to the differences in roughness length (which are related to differences in gravity wave shape as discussed in the following section) and to differences in wave–wave interaction related to the orbital velocity of the dominant waves. More steeply sloped waves have greater orbital velocities. The orbital velocity of the dominant waves reduces the wind shear related to the capillary wave riding on these waves and, hence, acts to reduce the stress (Bourassa et al. 1999). This mechanism causes a greater reduction of stress on growing (i.e., more steeply sloped) waves and, hence, reduces the phase speeds calculated with (16). However, removing this form of wave–wave interaction from the model does not qualitatively change the dependence of  $U_{\text{cutoff}}$  on  $W$ . The dominant influence is the change in roughness length related to the differences in wave shape.

### b. Wave shape and roughness length

It has been observed that the drag coefficient ( $u_*^2/U^2$ ), and hence roughness length, tends to decrease as the significant wave height decreases (W. Peirson 1997, per-

sonal communication regarding observations by M. A. Donelan). This observation is often considered contradictory to common sense; however, it can be explained with this coupled flux and sea state model. Consider a departure from the equilibrium value of  $H_s$  without a change in  $U_{10}$ :  $H_s > H_s(U_{\text{eq}})$  is consistent with falling seas ( $W < 1$ ), and  $H_s < H_s(U_{\text{eq}})$  is consistent with rising seas ( $W > 1$ ). For a specific wind speed, the modeled drag coefficients are larger for growing seas than for falling seas, consistent with observations in question. However, this consistency does not clearly explain why a drag coefficient decreases as significant wave height increases. The answer is related to the shape of the waves: significant wave height is not the only characteristic that changes. The wavelength of the dominant waves ( $\lambda$ ) changes more rapidly than  $H_s$ , causing the significant slope ( $H_s/\lambda$ ) to decrease as  $H_s$  increases (Figs. 4b,c). The drag coefficient decreases as  $H_s$  increases because the wave field of a falling sea is smoother than the wave field of a growing sea.

### c. Fetch limited conditions

In the past decade, research interests have shifted from the open ocean to the nearshore environment. Therefore, the importance of limited fetch and duration limited conditions ( $W > 1$ ) have increased in interest. The effect of fetch can be described in terms of  $W$ : for very short fetch  $U(H_s) > U_{\text{eq}}$  and  $W > 1$ , and as the fetch increases  $U(H_s) \rightarrow U_{\text{eq}}$  and  $W \rightarrow 1$ . The relevance of nonequilibrium conditions is likely to become increasingly important as the understanding of wave–wave and air–sea interaction mechanisms increases, and remote sensing allows calculation of short timescale fluxes. Accurate simulations of wave age for duration-limited situations and swell are important in the modeling of fluxes and upper-ocean mixing (Bourassa 2000).

Without high temporal resolution satellite observations of sea state, the fetch problem is unlikely to be solved without the consideration of wave field evolution. Coupling a wave evolution model with the BVW model would allow wave height and  $W$  (and/or another growth parameter) to be determined as a function of time. The advantages of such a coupled model would be tremendous in that it would allow fetch to be considered in the classic sense (the distance downwind from land), as well as modeling open-ocean evolution of wave characteristics due to rising or falling winds (duration limited conditions). Several of the difficulties in coupling these models have already been discussed. The evolution models are spectral models, and for low winds (more precisely, for small dominant phase speeds) there is a significant difference between the BVW and P–M peak periods. Another problem is that the spectral models do not consider atmospheric stability, which has an effect on the capillary cutoff. A third problem is that the value of  $U(H_s)/c_p$  for conditions of local equilibrium is assumed to equal unity in spectral models but is found

herein to be  $0.32/\kappa$  ( $\approx 0.81$ ). Additionally, flux models may have to consider swell from multiple directions and the influences of short-term variability in the wind. The inconsistencies between flux models and wave evolution models must be overcome before they can be combined to model the effects of fetch.

## 6. Conclusions

A sea state parameterization with a nonarbitrary wave age has been developed. This model is extremely versatile in that it is not restricted to conditions of neutral atmospheric stability or local wind-wave equilibrium. The model's significant wave height and period of the dominant waves are quantitatively validated for conditions of local wind-wave equilibrium. The model is qualitatively validated for nonequilibrium conditions. The model is sensitive to the ratio of the mean wind speed at the significant wave height to the phase speed of the dominant waves. This ratio is found to be 0.81 for conditions of local equilibrium, which differs from the often assumed value of unity. This sea state parameterization provides a method for determining the wave age and related wave and flux characteristics in a physically consistent and nonarbitrary manner.

Differences in the model's equilibrium values of  $H_s(U_{10})$  and  $T_p(U_{10})$ , in comparison to an extrapolation of the Pierson-Moskowitz results are explained in terms of the influences of capillary waves and surface tension. These differences are insignificant for high wind speeds ( $U_{10} > 13 \text{ m s}^{-1}$ ), but increase as the wind speed decreases toward the capillary cutoff. For  $U_{10} < 4 \text{ m s}^{-1}$ , the changes in  $H_s$  and  $T_p$  are large and can exceed 50% near the capillary cutoff. These changes may prove significant in wave models with the period based on the Pierson-Moskowitz relation, which was developed for strong winds and fully developed seas. The model periods are somewhat validated with observations from two field experiments.

The significant wave height decreases and the significant slope increases as the magnitude of the wind in excess of equilibrium increases. This result is consistent with observations of decreasing drag coefficient with increasing significant wave heights (for constant wind speeds), and offers the first explanation for such observations.

*Acknowledgments.* We thank John Snow for helpful discussions, and anonymous reviewers for constructive comments. We thank Chris Fairall for providing the SCOPE data, and Will Drennan for providing the SWADE data. This research was primarily supported by the National Aeronautics and Space Administration under Grant NAG8-836, with partial support from the National Science Foundation under Grant ATM-9200534. Both grants were issued to Dr. Dayton Vincent at Purdue University. COAPS receives its base funding from the Secretary of Navy Grant from ONR to James J. O'Brien.

Current funding for MAB is from the NASA JPL NSCAT and OVWST Projects.

## REFERENCES

- Beljaars, A. C. M., and A. A. M. Holtslag, 1991: Flux parameterization over land surfaces for atmospheric models. *J. Appl. Meteor.*, **30**, 327–341.
- Benoit, R., 1977: On the integral of the surface layer profile-gradient functions. *J. Appl. Meteor.*, **16**, 859–860.
- Bourassa, M. A., 2000: Shear-stress model for the aqueous boundary layer near the air-sea interface. *J. Geophys. Res.*, **105**, 1167–1176.
- , D. G. Vincent, and W. L. Wood, 1999: A flux parameterization including the effects of capillary waves and sea state. *J. Atmos. Sci.*, **56**, 1123–1139.
- Brutsaert, W. A., 1982: *Evaporation into the Atmosphere*. Reidel, 299 pp.
- Byushev, V. I., and O. A. Kuznetsov, 1969: Stuktrunye kharakteristiki atmosfernoï turbulentnosti v privodnom sloe nad otkrytym okeanom. *Izv. Akad. Navk USSR, Fiz. Atmos. Okeana*, **5**, 327–332.
- Chalikov, D. V., 1978: The numerical simulation of wind-wave interaction. *J. Fluid Mech.*, **87**, 561–582.
- , 1986: Numerical simulation of the boundary layer above waves. *Bound.-Layer Meteor.*, **34**, 63–98.
- , and V. K. Makin, 1991: Models of the wave boundary layer. *Bound.-Layer Meteor.*, **63**, 65–68.
- Charnock, H., 1955: Wind stress on a water surface. *Quart. J. Roy. Meteor. Soc.*, **81**, 639–640.
- Chou, S.-H., 1993: A comparison of airborne eddy correlation and bulk aerodynamic methods for ocean-air turbulent fluxes during cold-air outbreaks. *Bound.-Layer Meteor.*, **64**, 75–100.
- Csanady, G. T., 1985: Air-sea momentum transfer by means of short crested wavelets. *J. Phys. Oceanogr.*, **15**, 1486–1501.
- Donelan, M. A., 1990: Air-sea interactions. *The Sea*. Vol. 9: *Air-Sea Interaction*. B. LeMahaute and D. M. Hanes, Eds., Wiley and Sons, 239–292.
- , F. W. Dobson, S. D. Smith, and R. J. Anderson, 1993: On the dependence of sea-surface roughness on wave development. *J. Phys. Oceanogr.*, **23**, 2143–2149.
- , W. M. Drennan, and K. B. Katsaros, 1997: The air-sea momentum flux in conditions of wind sea and swell. *J. Phys. Oceanogr.*, **27**, 2087–2099.
- Fairall, C. W., E. F. Bradley, D. P. Rogers, J. B. Edson, and G. S. Young, 1996: Bulk parameterizations of air-sea fluxes for Tropical Ocean-Global Atmosphere Coupled Ocean-Atmosphere Response Experiment. *J. Geophys. Res.*, **101**, 3747–3764.
- Geernaert, G. L., K. B. Katsaros, and K. Richter, 1986: Variation of the drag coefficient and its dependence on sea state. *J. Geophys. Res.*, **91**, 7667–7697.
- Günther, H., and Coauthors, 1992: Implementation of a third generation ocean wave model at the European Centre for Medium-Range Weather Forecasts. ECMWF Tech. Rep. 68, 34 pp.
- Hasselmann, K., D. B. Ross, P. Müller, and W. Sell, 1976: A parametric wave prediction model. *J. Phys. Oceanogr.*, **6**, 200–208.
- Hay, J. S., 1955: Some observations of air flow over the sea. *Quart. J. Roy. Meteor. Soc.*, **81**, 307–319.
- Hsu, S. A., 1974: A dynamic roughness equation and its application to wind stress determination at the air-sea interface. *J. Phys. Oceanogr.*, **4**, 116–120.
- Huang, N. E., C. Tung, and S. R. Long, 1990: Wave spectra. *The Sea*. Vol. 9: *Air-Sea Interaction*, B. LeMahaute and D. M. Hanes, Eds., John Wiley and Sons, 197–238.
- Janssen, P. A. E. M., 1982: Quasi-linear approximations for the spectrum of wind-generated water waves. *J. Fluid Mech.*, **117**, 493–506.
- , 1989: Wave-induced stress and the drag of airflow over sea waves. *J. Phys. Oceanogr.*, **19**, 745–754.

- , 1991: Quasi-linear theory of wind-wave generation applied to wave forecasting. *J. Phys. Oceanogr.*, **21**, 1631–1642.
- Jeffereys, H., 1925: On the formation of water waves by wind. *Proc. Roy. Soc. London*, **A107**, 189–206.
- Jenkins, A. D., 1992: A quasi-linear eddy viscosity model for the flux of energy and momentum to wind waves, using conservation-law equations in a curvilinear coordinate system. *J. Phys. Oceanogr.*, **22**, 843–858.
- , 1993: A simplified quasi-linear model for wave generation and air–sea momentum flux. *J. Phys. Oceanogr.*, **23**, 2001–2018.
- Kawai, S., 1981: Visualization of airflow separation over wind-wave crests under moderate wind. *Bound.-Layer Meteor.*, **21**, 93–104.
- , 1982: Structure of air flow separation over wind wave crests. *Bound.-Layer Meteor.*, **23**, 502–522.
- Kitaigorodskii, S. A., 1961: Application of the theory of similarity to the analysis of wind generated wave motion as a stochastic process. *Izv. Akad. Nauk SSSR, Ser. Geofiz.*, **1**, 105–117; English translation, **1**, 73–80.
- , 1970: The physics of air–sea interaction. Israel Program for Scientific Translations, Jerusalem, Israel, 237 pp.
- Komen, G. L., L. Cavaleri, M. Donelan, K. Hasselmann, S. Hasselmann, and P. A. E. M. Janssen, 1994: *Dynamics and Modelling of Ocean Waves*. Cambridge University Press, 532 pp.
- Kondo, J., 1975: Air–sea bulk transfer coefficients in diabatic conditions. *Bound.-Layer Meteor.*, **9**, 91–112.
- Kusaba, T., and A. Masuda, 1988: The roughness height and drag law over the water surface based on the hypothesis of local equilibrium. *J. Phys. Oceanogr. Soc. Japan*, **44**, 200–214.
- Large, W. G., J. Morzel, and G. B. Crawford, 1995: Accounting for surface wave distortion of the marine wind profile in low-level ocean storms wind measurements. *J. Phys. Oceanogr.*, **25**, 2959–2971.
- Liu, W. T., K. B. Katsaros, and J. A. Businger, 1979: Bulk parameterization of air–sea exchanges of heat and water vapor including the molecular constraints at the interface. *J. Atmos. Sci.*, **36**, 1722–1735.
- Maat, M., C. Kraan, and W. A. Oost, 1991: The roughness of wind waves. *Bound.-Layer Meteor.*, **54**, 89–103.
- Makin, V. K., 1980: Numerical simulation of the structure of the near water atmospheric layer in the presence of a developed sea. *Oceanology*, **20**, 139–142.
- , 1982: Numerical studies of wind–wave interaction. *Oceanography*, **27**, 128–132.
- , 1987: Wavelike momentum fluxes in boundary layer above sea waves. *Oceanology*, **27**, 525–530.
- , and Ye. G. Panchenko, 1986: Numerical studies of energy transfer from the wind to waves along a limited fetch. *Izv. Acad. Sci. USSR, Atmos. Oceanic Phys.*, **22**, 163–165.
- Miles, J. W., 1957: On the generation of surface waves by turbulent shear flows, Part 2. *J. Fluid Mech.*, **6**, 568–582.
- Nikuradse, J., 1933: *Stromungsgesetze in rauhen Rohren*. Verin Deutscher Ingenieure Forschungsheft 361, 22 pp. English Translation, NACA Tech. Memo. 1292, National Advisory Commission for Aeronautics, 1950.
- Perrie, W., and B. Toulany, 1990: Fetch relations for wind-generated waves as a function of wind-stress scaling. *J. Phys. Oceanogr.*, **20**, 1666–1681.
- Phillips, O. M., 1977: *The Dynamics of the Upper Ocean*. 2d ed. Cambridge University Press, 336 pp.
- Pierson, W. J., Jr., and L. Moskowitz, 1964: A proposed spectral form for fully developed wind seas based on similarity theory of S. A. Kitaigorodskii. *J. Geophys. Res.*, **69**, 5181–5190.
- Smith, S. D., 1980: Wind stress and heat flux over the ocean in gale force winds. *J. Phys. Oceanogr.*, **10**, 709–726.
- , 1988: Coefficients for sea surface wind stress, heat flux, and wind profiles as a function of wind speed and temperature. *J. Geophys. Res.*, **93**, 15 467–15 472.
- , and Coauthors, 1992: Sea surface wind stress and drag coefficients: The HEXOS results. *Bound.-Layer Meteor.*, **60**, 109–142.
- Stewart, R. W., 1974: The air–sea momentum exchange. *Bound.-Layer Meteor.*, **6**, 151–167.
- Stull, R. B., 1988: Measurement and simulation. *An Introduction to Boundary Layer Meteorology*, Kluwer Academic, 405–440.
- Toba, Y. N., 1972: Local balance in the air–sea boundary-layer processes. I. On the growth of wind waves. *J. Oceanogr. Soc. Japan*, **28**, 109–120.
- , N. Ida, H. Kawamura, N. Ebuchi, and I. S. F. Jones, 1990: Wave dependence of sea-surface wind stress. *J. Phys. Oceanogr.*, **20**, 705–721.
- Ursell, F., 1956: Wave generation by wind. *Surveys in Mechanics*, G. K. Batchelor and R. M. Davies, Eds., Cambridge University Press, 216–249.
- Wu, J., 1968: Laboratory studies of wind–wave interactions. *J. Fluid Mech.*, **34**, 91–111.
- , 1980: Wind-stress over sea surfaces near neutral conditions—A revisit. *J. Phys. Oceanogr.*, **10**, 727–740.
- Yelland, M. J., B. I. Moat, P. K. Taylor, R. W. Pascal, J. Hutchings, and V. C. Cornell, 1998: Wind stress measurements from the open ocean corrected for airflow distortion by the ship. *J. Phys. Oceanogr.*, **28**, 1511–1526.